Basic Res Cardiol (2011) 106:879–895
DOI 10.1007/s00395-011-0191-y

ORIGINAL CONTRIBUTION

Opposing effects of monomeric and pentameric C-reactive protein on endothelial progenitor cells

I. Ahrens · H. Domeij · S. U. Eisenhardt · D. Topcic · M. Albrecht · E. Leitner · K. Viitaniemi · J. B. Jowett · M. Lappas · C. Bode · I. Haviv · K. Peter

Received: 21 September 2010 / Revised: 12 April 2011 / Accepted: 29 April 2011 / Published online: 12 May 2011

Abstract C-reactive protein (CRP) has been linked to the pathogenesis of atherosclerosis. The dissociation of native, pentameric (p)CRP to monomeric (m)CRP on the cell membrane of activated platelets has recently been demonstrated. The dissociation of pCRP to mCRP may explain local pro-inflammatory reactions at the site of developing atherosclerotic plaques. As a biomarker, pCRP predicts cardiovascular adverse events and so do reduced levels and function of circulating endothelial progenitor cells (EPCs). We hypothesised that mCRP and pCRP exert a differential effect on EPC function and differentiation. EPCs were treated with mCRP or pCRP for 72 h, respectively. Phenotypical characterisation was done by flow cytometry and immunofluorescence microscopy, while the effect of mCRP and pCRP on gene expression was examined by whole-genome gene expression analysis. The functional capacity of EPCs was determined by colony forming unit (CFU) assay and endothelial tube formation assay. Double staining for acetylated LDL and ulex lectin significantly decreased in cells treated with pCRP. The length of tubuli in a matrigel assay with HUVECs decreased significantly in response to pCRP, but not to mCRP. The number of CFUs increased after pCRP treatment. RNA expression profiling demonstrated that mCRP and pCRP cause highly contradictory gene regulation. Interferon-responsive genes (IFI44L, IFI44, IFI27, IFI 6, MX1, OAS2) were among the highly up-regulated genes after mCRP, but not after pCRP treatment. In conclusion, EPC phenotype, genotype and function were differentially affected by mCRP and pCRP, strongly arguing for differential roles of these two CRP conformations. The up-regulation of interferon-inducible genes in response to mCRP may constitute a mechanism for the local regulation of EPC function.

Keywords CRP · mCRP · EPC · Cardiovascular disease · Gene array · Interferon-alpha

Ahrens and Domeij have contributed equally to this work.

Electronic supplementary material The online version of this article (doi:10.1007/s00395-011-0191-y) contains supplementary material, which is available to authorized users.

I. Ahrens (✉) · M. Albrecht · C. Bode
Department of Cardiology and Angiology, University Hospital Freiburg, Hugstetter Street 55, 79106 Freiburg, Germany
e-mail: ingo.ahrens@uniklinik-freiburg.de

I. Ahrens · H. Domeij · D. Topcic · M. Albrecht · E. Leitner · K. Viitaniemi · K. Peter
Atherothrombosis and Vascular Biology, Baker IDI Heart and Diabetes Institute, Melbourne, Australia

S. U. Eisenhardt
Department of Plastic and Hand Surgery, University Hospital Freiburg, Freiburg, Germany

J. B. Jowett · I. Haviv
The Blood and DNA Profiling Facility, Baker IDI Heart and Diabetes Institute, Melbourne, Australia

M. Lappas
Department of Obstetrics and Gynaecology, Mercy Hospital for Women, University of Melbourne, Melbourne, Australia

Introduction

C-reactive protein (CRP) is an acute phase protein that consists of five non-covalently linked subunits forming a disc-shaped pentamer (pCRP) with a molecular weight of 115 kDa. The serum level of pCRP has been established as an independent risk factor for cardiovascular events [23, 51, 71]. We recently demonstrated the dissociation of pCRP to monomeric (m)CRP on the cell membrane of

activated platelets and the deposition of mCRP in atherosclerotic plaques, thereby suggesting a causal link between localised inflammation, C-reactive protein and atherosclerosis [15, 17]. In addition to our recent findings, evidence from other studies points towards a differential effect of mCRP and pCRP on the activation of platelets and leukocytes [16, 34, 40], which are known key players involved in the initiation of atherosclerotic plaque development [26].

While elevated serum levels of C-reactive protein are predictive of adverse cardiovascular events [23, 51, 71], decreased numbers of circulating endothelial progenitor cells (EPCs) and impaired function of EPCs have been described [18, 31, 45, 48, 55, 67, 68], thereby generating the hypothesis that C-reactive protein might have a negative effect on EPC number and function. In addition, in vitro experiments have shown that pCRP reduces the number of differentiated EPCs along with a reduction in EPC-mediated endothelial tube formation [64]. Furthermore, a recent study by the same group demonstrated a dose-dependent increase in pCRP-induced formation of reactive oxygen species and apoptosis in EPCs [19].

However, the effects of C-reactive protein are versatile and still not fully understood. It appears that inflammation accompanied by elevated levels of C-reactive protein in general does not necessarily lead to decreased levels of circulating EPCs [20, 47]. In fact, the EPC number may even be elevated [20].

The recent description of the dissociation of pCRP to mCRP on cell membranes thereby generating two biologically distinct conformations of C-reactive protein [15, 28] prompted us to examine whether mCRP and pCRP have a differential effect on EPC differentiation and function.

The term EPC has initially been applied to describe a cell population possessing the ability to regenerate damaged endothelium and contribute to the development of new vessel structures (EPC) [3]. Investigations into the different purification and culturing methods have sparked an ongoing discussion about a more differentiated definition of these progenitor cells with regenerative capacities [13, 24, 50, 53, 58, 61, 62, 69]. The new definition allows a crude separation into early outgrowth EPC or pro-angiogenic cells [13] and endothelial outgrowth cells (EOCs) also described as endothelial colony forming cells (ECFCs) [24, 61, 69]. The cells that were used in the current study were derived from $CD34^+$ selected human umbilical cord blood mononuclear cells. After in vitro expansion, the cells were differentiated into early outgrowth EPCs [1]. CD34 is a hematopoietic progenitor cell (HPC) marker, which has been linked to the term EPC throughout the majority of the available EPC literature [63, 66]. Therefore, for simplification purposes we use the term HPC to describe the $CD34^+$-purified cells and the general term EPC to describe the cells that were used for the experiments throughout our study.

$CD34^+$ cells purified by positive selection from human cord blood samples were expanded in vitro and thereafter differentiated into EPCs in the presence or absence of mCRP or pCRP, respectively. pCRP and mCRP showed differential effects on survival, differentiation and function of EPCs. In addition, whole-genome gene expression analysis revealed a highly differentially and opposing gene expression pattern in response to treatment with the two isoforms of CRP. Interferon-responsive genes (IFI44L, IFI44, IFI27, IFI 6, MX1, OAS2) were among the highly up-regulated genes in response to mCRP, but not pCRP treatment of EPCs.

Materials and methods

Isolation and expansion of $CD34^+$ cells

Mononuclear cells (MNCs) were isolated from human umbilical cord blood (HUCB) obtained from healthy donors following normal full-term deliveries after their written informed consent. Ethics approval was granted by the Human Research Ethics Committee, Mercy Health, Mercy Hospital for Women, Melbourne, Australia (Project number R08/24).

HUCB was collected in 50 ml Falcon tubes (BD Bioscience, NJ, USA) containing 15 ml of the anticoagulant citrate phosphate dextrose. After collection, HUCB was diluted 1:3 in isolation buffer (PBS, 0.1% BSA, 0.6% citrate, pH 7.4). MNCs were isolated from the diluted HUCB by density gradient centrifugation, whereby 20 ml of diluted HUCB were layered onto 15-ml Ficoll-Paque™ (GE Healthcare, Chalfont, UK) and centrifuged for 30 min at $800\times g$. Thereafter, the interphase containing MNCs was collected and washed with an equal amount of isolation buffer, followed by centrifugation for 30 min at $500\times g$. The washed MNCs were then subjected to magnetic beads-based selection of $CD34^+$ cells using Dynal® CD34 Progenitor Cells Selection System (Invitrogen, Oslo, Norway) following the manufacturer's recommendation. The number of positively selected $CD34^+$ cells, the haematopoietic progenitor cells (HPC), was assessed in a Neubauer haemocytometer and the purity (>90%) of the $CD34^+$ cells evaluated by flow cytometry.

The cord blood-derived $CD34^+$ HPCs were cultured at a density of 3–5 $\times$ 10^4 cells/400 µl/1.8 cm^2 in a humidified incubator at 37°C with 5% CO_2. The cells were cultured for 7 days in serum-free StemSpan® medium (StemCell Technologies, Vancouver, Canada) during the initial expansion period and supplemented with 1% penicillin–streptomycin (Sigma-Aldrich, St. Louis, USA) and

recombinant human (rh) Flt-3 ligand (100 ng/ml), rh stem cell factor (100 ng/ml), rh IL-3 (20 ng/ml) and rh IL-6 (20 ng/ml), all purchased from StemCell Technologies. Thereafter, the HPCs were cultured (3×10^5–1×10^6/1.5 ml/9.6 cm^2) for an additional 3 days in endothelial cell growth medium-2 (EGM-2) containing FBS (2%), hydrocortisone, hFGF, VEGF, R^3-IGF-1, ascorbic acid, hEGF, gentamicin, amphotericin-B and heparin (Lonza, Basel, Siwtzerland).

Treatment of EPCs with monomeric and pentameric CRP

pCRP (Chemicon, Temecula, USA) and mCRP were prepared as described previously [15]. The expanded HPCs described above were collected and transferred to fibronectin (10 μg/ml) (Sigma-Aldrich)-coated plates, cultured and differentiated into EPCs for 3 days in fresh EGM-2 media in the presence or absence of mCRP (1, 5 or 25 μg/ml) or pCRP (1, 5 or 25 μg/ml), respectively. A control group of HPCs treated with EGM-2 media containing PBS (diluted 1:40) was also included.

Cell viability assays

Phosphatidylserine translocation (annexin V binding)

The binding of annexin V to phosphatidylserine was determined using FITC-conjugated annexin V (BD Biosciences, San Jose, CA, USA). In brief, the EPCs were washed in annexin-binding buffer (10 mM HEPES, 140 mM NaCl, 2.5 mM $CaCl_2$, pH 7.4) and thereafter incubated with annexin V-FITC at RT for 15 min. After additional washing in annexin-binding buffer, the cells were analysed for annexin V-FITC binding in a FACSCalibur TM flow cytometer using CellQuest software (Becton and Dickinson, San Jose, CA, USA). Between 10,000 and 20,000 events per test were acquired. A negative control with unstained cells was included for each treatment.

CytoTox-Glo™ cytotoxicity assay

The relative viability of EPCs treated with mCRP (1, 5, or 25 μg/ml), pCRP (1, 5, or 25 μg/ml) or PBS was analysed using the CytoTox-Glo™ cytotoxicity assay (Promega, Madison, WI, USA) following the manufacturer's recommendations. In brief, EPCs were added to a 96-well luminescence plate at a concentration of 10,000 cells/well in a volume of 100 μl of EGM-2. Thereafter, to detect protease activity that had been released from dead cells, 50 μl of alanyl-alanyl-phenylalanyl-aminoluciferin luminogenic peptide substrate (AAF-Glo™ Substrate) mix was added to the wells and incubation was carried out for 15 min at RT. The plate was measured in a 96-well plate luminometer. Immediately after measurement of dead cells by luminescence, the EPCs were exposed to a lysis buffer containing digotinin for 15 min at RT and the luminescence was measured again. The number of viable cells was determined by subtracting the number of dead cells from the total cell count. A no-cell background control was included in the assay.

Uptake of acetylated LDL and binding of ulex lectin

To investigate the endothelial progenitor characteristics of the EPCs, binding of ulex lectin and uptake of Dil-labelled acetylated LDL (AcLDL) by the cells were analysed by dual staining of the cells at 37°C in PBS.

After expansion, the cells were seeded on a fibronectin-coated 24-well plate with a density of 3×10^5cells/0.5 ml/1.8 cm^2 and cultured in EGM-2 for 3 days in the presence or absence of mCRP, pCRP or PBS. Thereafter, cells were washed twice with PBS at 37°C. The cells were then incubated with Dil-AcLDL (6 μg/ml) (Invitrogen, Carlsbad, USA) for 1 h at 37°C in the dark. Thereafter, the cells were washed twice with PBS at 37°C and incubated with FITC-conjugated ulex lectin (10 μg/ml) (Sigma-Aldrich, St. Louis, USA) for 1 h at 37°C in the dark. After two final washing steps with PBS at 37°C, the cells were fixed with 0.3 ml CellFIX solution (BD Biosciences, NJ, USA), and subsequently analysed for uptake of Dil-AcLDL and binding of FITC-ulex lectin using an Olympus 1X81 inverted fluorescence microscope.

The effect of mCRP and pCRP on functional characteristics of EPCs

The EPCs treated with mCRP or pCRP were studied using colony forming assay (CFU-Hill) and Matrigel™ tube formation assay.

Colony forming unit (CFU) assay

Culture of CFU-Hill colonies (StemCell Technologies) was performed according to the manufacturer's recommendations with the exception that we used ten times less cells (5×10^5 cells/well) and in vitro differentiated cord blood-derived EPCs instead of freshly prepared MNCs. In brief, after 72 h of culture on fibronectin in EGM-2 media in the presence or absence of mCRP or pCRP, the cells were collected and counted. The collected cells were then cultured (5×10^5 cells/1.5 ml/9.6 cm^{-2}) on fibronectin precoated 6-well plates (BD Biosciences) in EndoCult® liquid medium containing EndoCult supplements (StemCell Technologies). After 2 days, the non-adherent cells were

collected and transferred to fibronectin pre-coated 24-well plates (BD Biosciences) at a density of 3×10^5 cells/ml/1.8 cm^2. After a further 3 days of culture, the cells were washed twice with PBS, fixed with methanol, and the colonies were visualised with Giemsa staining (Gibco, Carslbad, USA), following the manufacturer's recommendations. The number of colonies per well was counted with an inverted microscope (Olympus CKX41).

Endothelial tube formation assay

The capability of the mCRP- and pCRP-treated EPCs to support endothelial tube formation was assessed using Matrigel™ (BD Biosciences) coated 96-well plates and human umbilical vein endothelial cells (HUVECs) in early passages (P3-P6). In brief, wells of a 96-well plate were coated with 50 µl of ice-cold Matrigel™ followed by incubation at 37°C for 1 h. Thereafter, 100 µl of EGM-2 medium containing 25,000 HUVECs and 100 µl of EGM-2 containing 25,000 EPCs were added to the Matrigel™. Incubation was carried out for 16 h in a humidified atmosphere at 37°C in the presence of 5% CO_2. Tube formation was assessed with an inverted microscope (Olympus 1X81) and Cell^P imaging software (Olympus). Digital photomicrographs of each single well were taken at a 4× magnification and the total number of tubes, branching points, and the length of the tubes as well as the sum of the lengths of all tubes were calculated for each well.

Whole-genome gene expression analysis of mCRP and pCRP-treated EPCs

Total RNA was extracted from 2×10^6 EPCs after 72 h of culture in EGM-2 medium in the presence or absence of mCRP (1 µg/ml), pCRP (5 µg/ml) or PBS. The RNA was obtained using Qiagen® RNeasy protect mini kit™ following the manufacturer's instructions. RNA concentration and integrity was analysed by NanoDrop (Thermo Fischer Scientific, Waltham, USA) and MultiNA microchip electrophoresis (Shimadzu Biotech, Kyoto, Japan) according to the manufacturer's recommendations. Total RNA was amplified with the TotalPrep™ RNA Amplification Kit (Ambion, UK) and applied to Illumina® Human WG-6 v3.0 Expression BeadChip kits according to the manufacturer's instructions. Fluorescent bead intensity was transformed into gene expression level via Illumina Genome Studio, including quantile normalisation [27] and background subtraction. The exported reports were analysed on GeneSpring GX10, Partek GS and arraytools (http://linus.nci.nih.gov/pub/rsimon/ ArrayTools). Genes with a raw signal <250 and a detection confidence >0.8 in at least three arrays were filtered out, leaving 6,064 genes for further analysis. Whisker box plot was used to confirm the quintile normalisation eliminated systematic cross array variations in the overall dynamic range. Quality control of the samples and controlling for systematic bias were performed using principal component analysis and unsupervised hierarchical clustering to show that samples segregated according to treatment groups. Differentially expressed genes were selected based on a Bayesian "volcano plot" of expression fold change greater than twofold and significance p value of <0.05, including Benjamini Hochberg false discovery correction. Differential expression of the chosen genes across the treatment groups was assessed using supervised hierarchical clustering [14] that measures the proximity of distribution of samples and genes. The interpretation of the resulting gene lists was performed using gene ontology Web interface (http://david.abcc.ncifcrf.gov/), Gene Set Analysis [6], protein–protein interaction KEGG database [22] and Ingenuity Pathways Analysis [49].

Quantitative real-time PCR analysis

First-strand cDNA was synthesised using 350 ng of total RNA, obtained as described in the microarray section, and random primers in a 10 µl reverse transcriptase reaction mixture using TaqMan® Reverse Transcription Reagents (Applied Biosystems) following the manufacturer's recommendations. Quantitative real-time PCR assays were carried out with Applied Biosystems 7500 real-time PCR system using SYBR® Green Mastermix (Applied Biosystems, Carlsbad, USA). Primers were designed in-house and synthesised by GeneWorks (Hindmarsh, Australia). PCR amplification was performed in a 96-well plate with a final volume of 20 µl reaction mixture in each well. For each sample, 21 ng of cDNA was loaded in duplicates with 1× SYBR® Green Mastermix and 10 µM of the following primers for: Mx1 sense 5′-CACTGCGCAGGGACCGGAATT-3′ and anti-sense 5′-TCCTGTAGCCTCCGACCCAGAA-3′; OAS2 sense 5′-GCTCCCGGCCCACCAAACTA-3′ and anti-sense 5′-TGGGGGCAAAGACCCCTTTGG-3′; OAS3 sense 5′-GGACCCTGCAGTTGGGCAGT-3′ and anti-sense 5′-CCCATGTGGGGTCAGCTGGG-3′; IFIT3 sense 5′-ACCGGGACCCCAGCTTTTCAG-3′ and anti-sense 5′-AGCTGTGGAAGGATTTTCTCCAGGG-3′; IFI6 sense 5′-TCCGGGCTGAAGATTGCTTCTCTT-3′ and anti-sense 5′- ACTTTTTCTTACCTGCCTCCACCCC-3′; IFI44 sense 5′-GAGATGTGAGCCTGTGAGGTCCAA-3′ and anti-sense 5′TTTACAGGGTCCAGCTCCCACTCA-3′; IFI27 sense 5′- CCGTAGTTTTGCCCCTGGCC-3′ and anti-sense 5′-CATGGGCACAGCCGCCATG-3′; IFI44L sense 5′- ATGTGACTGGCCAAGCCGTAGT-3′ and anti-sense 5′TGCCCCATCTAGCCCCATAGTGT-3′; PROK2 sense 5′-TGGGAGACAGCTGCCATCCAC-3′ and anti-sense 5′-AGCCTGGCAGACATGGGCAA3′; DDIT3 sense 5′-TC

AGAGCTGGAACCTGAGGAGAGA-3′ and anti-sense 5′-ATGGGGAGTGGCTGGAACAAGC-3′. Relative expression of the genes was obtained using the differences in cycle threshold (Ct) between the sample and 18S ribosomal RNA (ΔC). The difference in gene expression for the treated samples compared to the PBS control samples was calculated (ΔΔCt) and the fold difference was calculated as 2ΔΔCt.

Treatment with human IFNα2A

The expanded HPCs were collected and transferred to fibronectin (10 μg/ml)-coated plates, cultured and differentiated into EPCs for 3 days in fresh EGM-2 media in the presence or absence of IFNα2A (0.1–10 ng/ml) (Sigma), mCRP (1 μg/ml) or pCRP (5 μg/ml), respectively. A control group of HPCs treated with EGM-2 media containing PBS (diluted 1:40) was also included. Changes in gene expression were determined using real-time PCR. In addition, uptake of AcLDL and binding of ulex lectin, CFU assay and endothelial tube formation assay were investigated as described above.

Statistical analysis

All experiments were performed with EPCs from at least three different donors, respectively. Mean and SD were used for descriptive statistics. Statistical analysis was performed using Sigma Stat. Differences between means were assessed by analysis of variance (ANOVA) and post hoc test was carried out according to Bonferroni. p values <0.05 were considered to be statistically significant.

Results

EPCs were treated with mCRP, pCRP or PBS for a period of 72 h in fibronectin-coated six-well plates (10 μg/ml). Thereafter EPC viability, phenotype and function were assessed. In addition, differences in gene expression profiles were assessed in EPCs derived from three different cord blood donors before and after mCRP, pCRP and PBS treatment, respectively.

Assessment of mCRP and pCRP toxicity

The effect of a 72-h treatment period of mCRP and pCRP on EPC viability was investigated using a cytotoxicity luminescence assay. First, the number of dead cells was measured and secondly the total number of cells was measured. The relative number of viable cells (relative live cell luminescence, RLU) obtained in the assay is demonstrated in Fig. 1a. There was no toxicity associated with mCRP treatment (1, 5, or 25 μg/ml for 72 h). In fact, mCRP significantly ($p < 0.05$–0.001) increased the viability/cell numbers in a dose-dependent manner (Fig. 1a). In accordance to mCRP, pCRP at the concentrations 1 and 5 μg/ml for 72 h was not toxic to the EPCs. However, at the concentration of 25 μg/ml, the viability of the cells was strongly reduced ($p < 0.001$, Fig. 1a). In addition to the luminescence-based cytotoxicity assay, which is based on protease activity released from cells through the loss of membrane integrity, the effect of mCRP and pCRP treatment on EPCs was also determined by annexin V binding. In accordance with the cytotoxicity assay, only pCRP at the concentration 25 μg/ml induced an increased binding of annexin V, thereby indicating a pro-apoptotic/necrotic effect on EPCs (Fig. 1b).

In the following descriptive and functional investigations, we focused on the comparison of 1 and 5 μg/ml mCRP and pCRP, respectively, to adjust for molarity of the pentameric structure of pCRP.

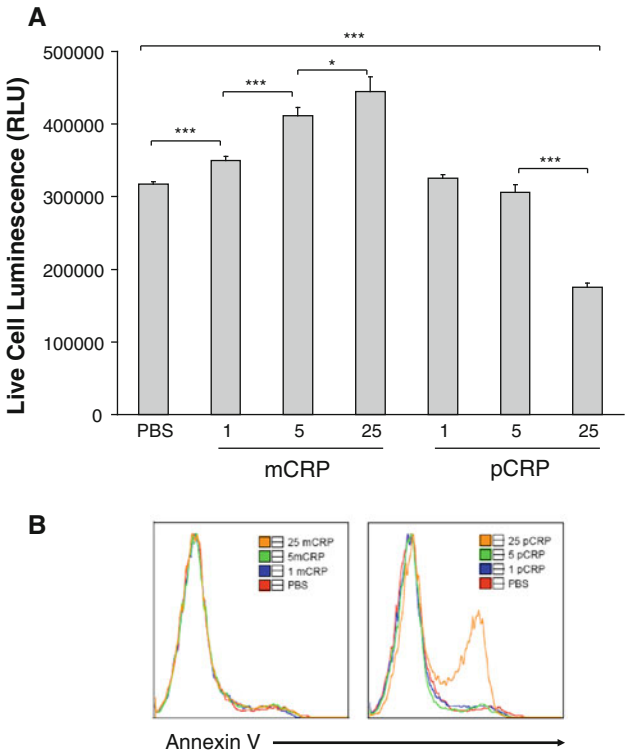

Fig. 1 Cytotoxicity assay after 72 h of EPC treatment with mCRP and pCRP. **a** Viable cells were measured by the CytoTox-Glo™ cytotoxicity assay. The *bars* represent the relative luminesce unit (RLU) calculated for the viable cells, i.e. dead cells deducted from total cells, mean and SD of $n = 3$. **b**. Histograms of one representative experiment showing the binding of the apoptosis marker Annexin V to EPCs using a FITC-labelled Annexin V antibody detected by flow cytometry

pCRP but not mCRP treatment decreased the number of AcLDL and ulex lectin double-positive cells

One phenotypic characteristic for EPCs is their ability to take up AcLDL and to bind ulex lectin. The uptake of AcLDL and the binding of ulex lectin were investigated by immunofluorescence staining using Dil-labelled AcLDL and FITC-labelled ulex lectin. The percentage of cells double positive for uptake of Dil-labelled AcLDL and binding of FITC-labelled ulex lectin after treatment with 1 μg/ml mCRP, 5 μg/ml pCRP and PBS was 36 ± 7, 42 ± 11 and 12 ± 3%, respectively (Fig. 2a). The percentage of double-positive cells indicating EPC phenotype was significantly decreased after pCRP treatment (12 ± 3%, $p < 0.05$, Fig. 2a). In contrast, EPCs treated with mCRP (1 μg/ml) were not affected and showed a similar percentage of double-positive cells compared to the PBS control.

Functional characteristics of EPCs are differentially affected by mCRP and pCRP

EPCs were treated with mCRP (1 μg/ml), pCRP (5 μg/ml) or PBS and then assessed for their ability to form colony forming units (CFU-Hill) and to support endothelial tube formation. Treatment of EPCs with pCRP significantly increased the number of CFUs (40 ± 5, $p < 0.001$), whereas mCRP (19 ± 2) did not affect the number of CFUs compared to PBS (25 ± 3) treated cells (Fig. 2b). The effect of mCRP (1 μg/ml) and pCRP (5 μg/ml) treatment on the ability of EPCs to support formation of endothelial tubuli in a co-culture with human umbilical

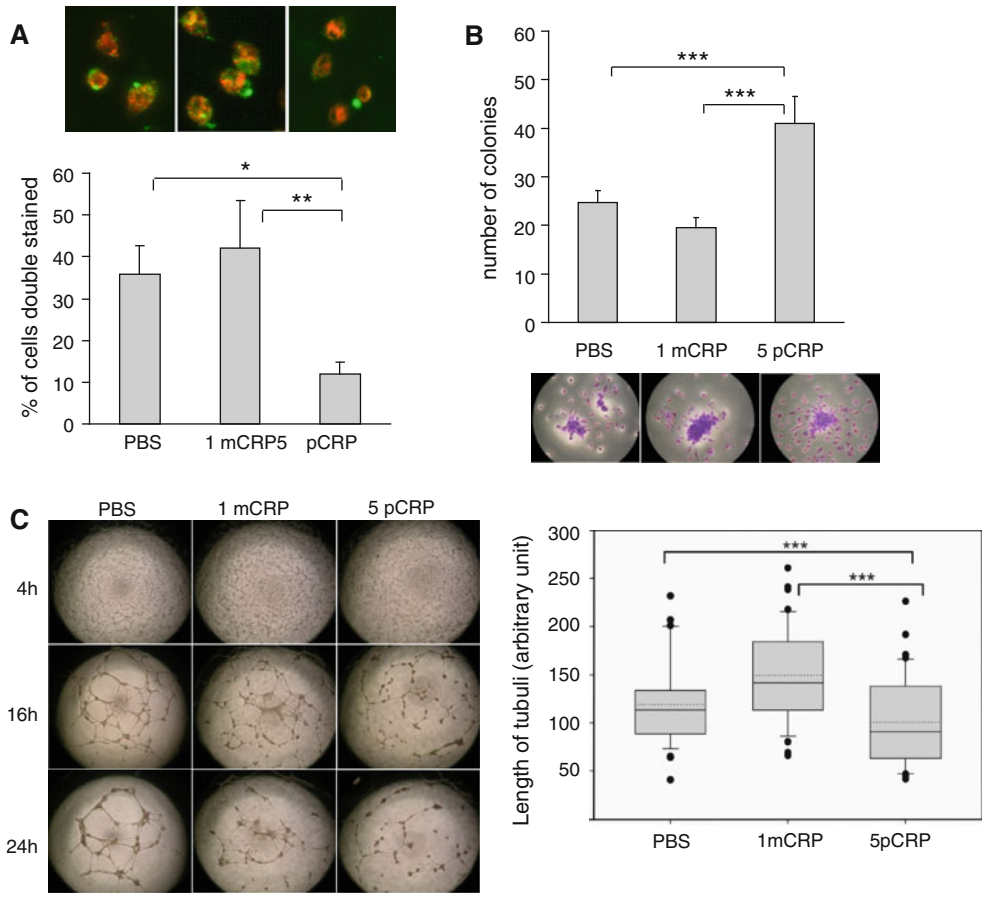

Fig. 2 The effect of mCRP (1 μg/ml) or pCRP (5 μg/ml) on phenotype and function of EPCs. **a** Binding of ulex lectin and uptake of AcLDL after 72 h of culture of EPCs in the presence or absence of mCRP or pCRP visualised with FITC-labelled ulex lectin and Dil-labelled AcLDL, respectively. The *photomicrographs* show a typical optical field from one representative experiment. The *bar graph* shows the percentage of double-positive cells, mean and SD of $n = 3$. **b** The number of colony forming units (CFU-Hill) visualised by Giemsa staining. The *bars* represent the total number of colonies per well in a 24-well plate, mean and SD of $n = 3$. **c** Endothelial tube formation assay after 72 h of culture of EPCs in the presence or absence of mCRP or pCRP. The treated EPCs were co-cultured with HUVECs for additional 4, 16 and 24 h, respectively. The photomicrographs show the results of a representative experiment. The length of the tubuli was assessed after 16 h. The *box* plot represents the mean (*dotted line*), median (*solid line*) and SD of three independent experiments

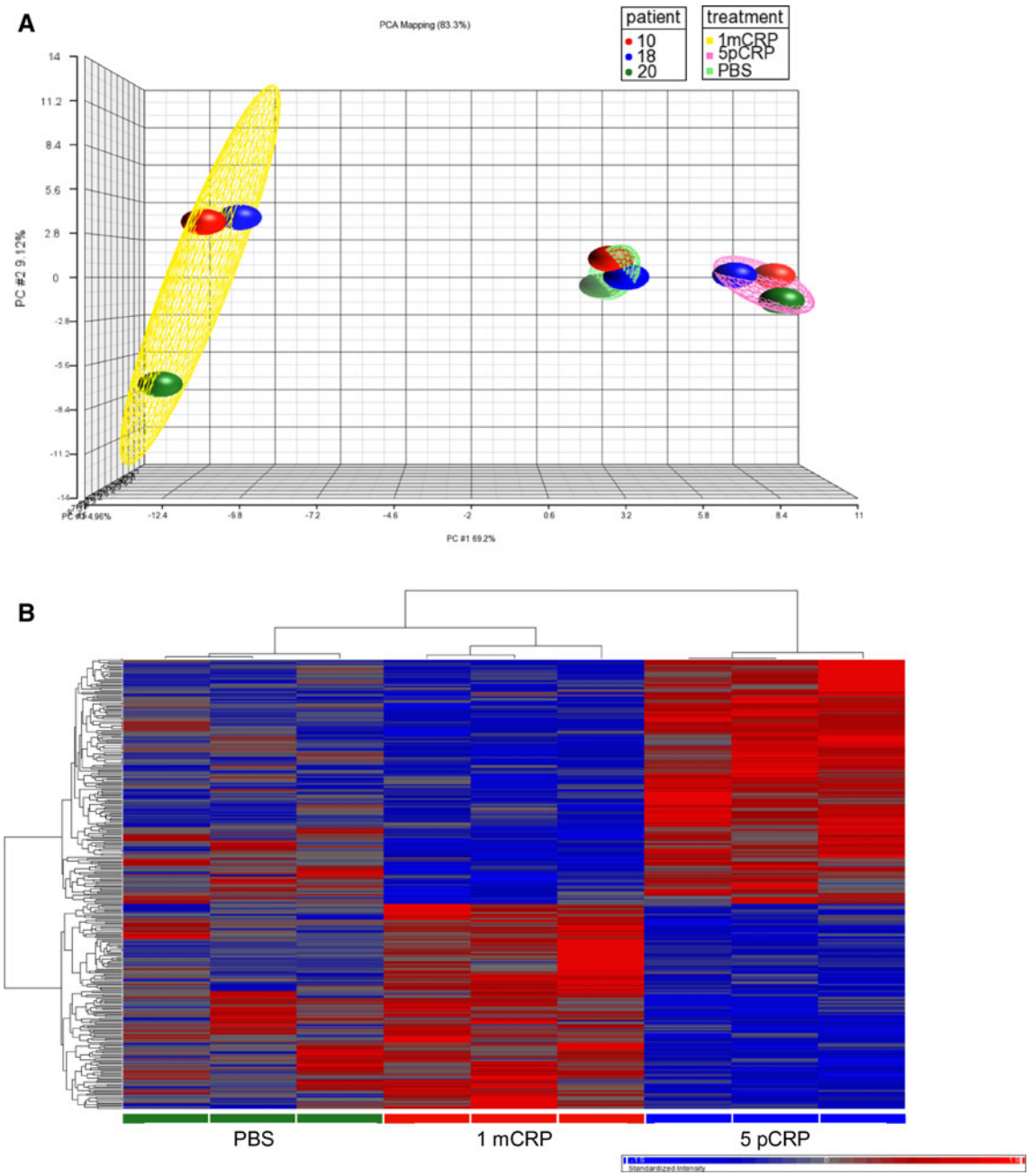

Fig. 3 **a** Principal component analysis (PCA) of the source of variation in the sample gene expression. This was an exploratory multivariate statistical technique that was used to simplify the complex microarray changes that occur in three individuals (patient 10, 18 and 20) and in response to different valency CRP. This is done by reducing the dimensionality of the data matrix by finding *r* new variables (that sum the expression of multiple genes into single axes); shown here are the average signal of each sample along the three-dimensional virtual space of the first three principal components. The plot clearly shows that the variation in gene expression is dominated by the CRP treatment and not the patient source. **b** Hierarchical clustering of the gene expression response to CRP valency; 320 differentially expressed genes are plotted according to their degree of respective co-expression. *Columns* represent samples, while *rows* represent genes. The treatment of each sample is listed at the *bottom*. The degree of correlation between genes (*left*) or samples (*top*) is plotted in a tree view fashion

vein endothelial cells was determined using a Matrigel™ assay. Tube formation occurred at 4 h of incubation on Matrigel™ and was maximal at 16 h of incubation (PBS-panel, Fig. 2c). After 24 h, the tube network started to break up, and this was facilitated when pCRP-treated EPCs were used (Fig. 2c). Neither mCRP nor pCRP affected the number of tubuli or branching points. However, the length of the tubuli was slightly increased by EPCs treated with

Table 1 Genes up- and down-regulated in EPCs treated with mCRP (1 μg/ml)

Gene symbol	Gene name	mCRP treatment		pCRP treatment	
		Fold change	*p* Value	Fold change	*p* Value
Up-regulated genes					
IFI44L	Interferon-induced protein 44-like	10.04	0.001	−2.36	0.61
MX1	Myxovirus (influenza virus) resistance 1	7.58	0.008	−2.68	0.46
OAS2	2′-5′-Oligoadenylate synthetase 2, 69/71kDA	6.84	0.001	−2.56	0.31
LY6E	Lymphocyte antigen 6 complex, locus E	6.18	0.003	−2.64	0.33
IFI27	Interferon, alpha-inducible protein 27	6.11	0.040	−2.52	0.63
IFI44	Interferon-induced protein 44	6.05	0.0005	−2.43	0.35
IFI6	Interferon, alpha-inducible protein 6	5.09	0.0004	−2.51	0.20
EPSTI1	Epithelial stromal interaction 1 (breast)	4.94	0.026	−2.06	0.94
OAS3	2′-5′-Oligoadenylate synthetase 3, 100 kDa	4.28	0.005	−2.90	0.10
IFIT3	Interferon-induced protein with tetratricopeptide repeats 3	3.87	0.048	−2.92	0.22
SAMD9L	Sterile alpha motif domain containing 9-like	3.73	0.002	−3.04	0.02
GLTPD2	Glycolipid transfer protein domain containing 2	3.65	0.009	−2.02	0.96
EIF2AK2	Eukaryotic translation initiation factor 2-alpha kinase 2	3.42	0.007	−2.14	0.65
DDX60	DEAD (Asp–Glu–Ala–Asp) box polypeptide 60	3.28	0.031	−2.24	0.57
SPINT4	Serine peptidase inhibitor, Kunitz type 4	3.23	0.026	−2.18	0.64
IRF7	Interferon-regulatory factor 7	3.14	0.032	−2.22	0.57
PARP9	Poly (ADP-ribose) polymerase family, member 9	3.10	0.031	−2.69	0.12
GPR87	G protein-coupled receptor 87	3.08	0.017	−2.09	0.77
RETSAT	Retinol saturase (all-trans-retinol 13, 14-reductase)	3.08	0.022	−2.30	0.38
CLDN4	Claudin 4	3.04	0.032	−2.27	0.46
IRF9	Interferon-regulatory factor 9	3.01	0.032	−2.53	0.18
OASL	2′-5′-Oligoadenylate synthetase-like	2.97	0.038	−2.46	0.23
PARP12	Poly (ADP-ribose) polymerase family, member 12	2.88	0.037	−2.50	0.17
STAT1	Signal transducer and activator of transcription 1	2.87	0.009	−2.29	0.24
HIST1H2AK	Histone cluster 1, H2ak	2.85	0.039	−2.25	0.43
PEX11A	Peroxisomal biogenesis factor 11 alpha	2.75	0.014	−2.50	0.06
POMT2	Protein-O-mannosyltransferase 2	2.61	0.003	−2.43	0.09
EPB41	Erythrocyte membrane protein band 4.1	2.56	0.014	−2.37	0.07
Down-regulated genes					
MLLT3	Myeloid/lymphoid or mixed-lineage leukaemia; translocated to, 3	−3.48	0.007	2.08	0.80
SOX1	SRY (sex determining region Y)-box 1	−3.25	0.002	2.04	0.86
SRD5A2	Steroid-5-alpha-reductase, alpha polypeptide 2	−3.16	0.008	2.55	0.10
ACSM1	Acyl-CoA synthetase medium-chain family member 1	−3.16	0.003	2.28	0.27
RNF133	Ring finger protein 133	−3.02	0.035	2.16	0.64
ROR1	Receptor tyrosine kinase-like orphan receptor 1	−2.99	0.032	2.03	0.92
ZEB1	Zinc finger E-box-binding homoeobox 1	−2.99	0.001	2.02	0.91
ZNF300	Zinc finger protein 300	−2.96	0.011	2.12	0.64
PRAMEF21	PRAME family member 21	−2.93	0.038	2.37	0.30
SRD5A3	Steroid 5 alpha-reductase-3	−2.87	0.024	2.26	0.37
RPL21	Ribosomal protein L21	−2.64	0.008	2.41	0.05
CARD18	Caspase recruitment domain family, member 18	−2.60	0.025	2.33	0.15
PCDHGB6	Protocadherin gamma subfamily B, 6	−2.50	0.021	2.57	0.01
GRIN1	Glutamate receptor, ionotropic	−2.42	0.008	2.49	0.004

Up- and down-regulated genes by mCRP ($n = 3$) compared to PBS-treated control EPCs were selected based on a Bayesian "volcano plot" of expression with a fold change in expression level greater than twofold, and a p value <0.05 as determined by student's t test

The fold change effect of pCRP treatment, as compared to PBS-treated control EPCs, for the differentially expressed genes was also determined

Table 2 Genes up- and down-regulated in EPCs treated with pCRP (5 μg/ml)

Gene symbol	Gene name	mCRP treatment		pCRP treatment	
		Fold change	*p* Value	Fold change	*p* Value
Up-regulated genes					
MFAP4	Microfibrillar-associated protein 4	3.60	0.0010	−2.03	0.855
RABGGTB	Rab geranylgeranyltransferase, beta subunit	3.51	0.0013	−2.05	0.793
FAM116B	Family with sequence similarity 116, member B	3.16	0.0040	−2.00	0.994
DDIT3	DNA damage-inducible transcript 3	3.08	0.0004	−2.07	0.578
PROK2	Prokinectin 2	3.08	0.0486	−2.13	0.690
RPL7A	Ribosomal protein L7a	3.05	0.0311	−2.43	0.215
PABPC4	Poly(A)-binding protein, cytoplasmic 4 (inducible form)	3.04	0.0042	−2.07	0.704
CELSR1	Cadherin, EGF LAG seven-pass G-type receptor 1	3.01	0.0104	−2.12	0.570
FRMD7	FERM domain containing 7	3.01	0.0499	−2.10	0.739
ZNF695	Zinc finger protein 695	3.00	0.0199	−2.04	0.859
HERC2	Hect domain and RLD2	2.99	0.0286	−2.00	0.998
RPL13L	Ribosomal protein L13 pseudogene 5	2.98	0.0094	−2.12	0.566
ZNF277	Zinc finger protein 277	2.96	0.0002	−2.11	0.325
LRAT	Lectin retinol acyltransferase	2.90	0.0157	−2.12	0.572
STAG3L4	Stromal antigen 3-like 4	2.87	0.0329	−2.25	0.368
ABHD14B	Abhydrolase domain containing 14B	2.86	0.0488	−2.17	0.554
AVPI1	Arginine vasopressin-induced 1	2.85	0.0062	−2.21	0.258
DYM	Dymeclin	2.82	0.0005	−2.05	0.652
ROM1	Retinal outer segment membrane protein 1	2.81	0.0099	−2.30	0.163
RAC3	ras-related C3 botulinum toxin substrate 3	2.81	0.0076	−2.10	0.558
CCDC104	Coiled-coil domain containing 104	2.81	0.0002	−2.15	0.164
SLC16A10	Solute carrier family 16, member 10	2.80	0.0082	−2.15	0.398
PHACTR1	Phosphatase and actin regulator 1	2.80	0.0079	−2.04	0.813
PCOLCE2	Procollagen C-endopeptidase enhancer 2	2.76	0.0379	−2.10	0.657
ZNF581	Zinc finger protein 581	2.75	0.0207	−2.11	0.602
CRP	C-reactive protein, pentraxin related	2.72	0.0400	−2.15	0.528
SIRPG	Signal-regulatory protein gamma	2.70	0.0129	−2.24	0.210
NNMT	Nicotinamide N-methyltransferase	2.70	0.0115	−2.07	0.685
EIF2A	Eukaryotic translation initiation factor 2A	2.69	0.0134	−2.22	0.249
FABP2	Fatty acid-binding protein 2, intestinal	2.69	0.0067	−2.13	0.411
RGMA	RGM domain family, member A	2.69	0.0146	−2.08	0.636
POLR1E	Polymerase (RNA) polypeptide E, 53 kDa	2.61	0.0358	−2.18	0.385
LETMD1	LETM1 domain containing 1	2.60	0.0168	−2.20	0.258
FTHL11	Ferritin, heavy polypeptide-like 11	2.59	0.0422	−2.25	0.261
CSNK2A2	Casein kinase 2, alpha prime polypeptide	2.57	0.0036	−2.27	0.061
CCDC140	Coiled-coil domain containing 140	2.53	0.0332	−2.17	0.346
PAX7	Paired box 7	2.49	0.0343	−2.25	0.190
ZFAND1	Zinc finger, AN 1-type domain 1	2.49	0.0175	−2.21	0.175
RAB39	RAB39, member RAS oncogene family	2.44	0.0350	−2.25	0.156
PCDHGB6	Protocadherin gamma subfamily B, 6	2.44	0.0115	−2.38	0.021
GRIN1	Glutamate receptor, inotropic, *N*-methyl D-aspartate 1	2.37	0.0041	−2.31	0.008
RPL21	Ribosomal protein L21	2.30	0.0474	−2.49	0.008
Down-regulated genes					
ABCA13	ATP-binding cassette, sub-family A (ABC1), member 13	−5.39	0.0009	2.02	0.931
LTF	Lactotransferrin	−5.11	0.0427	2.27	0.652
PDAP1	PDGFA associated protein 1	−5.04	0.0005	2.23	0.353

Table 2 continued

Gene symbol	Gene name	mCRP treatment		pCRP treatment	
		Fold change	*p* Value	Fold change	*p* Value
IFIT1	Interferon-induced protein with tetratricopeptide repeats 1	−4.39	0.0264	2.86	0.175
TXNIP	Thioredoxin-interacting protein	−3.75	0.0207	2.03	0.917
UGT1A3	UDP glucoronsyltransferase 1 family, polypeptide A3	−3.60	0.0453	2.05	0.891
RIMS3	Regulating synaptic membrane exocytosis 3	−3.47	0.0004	2.04	0.906
PKD2L1	Polycystic kidney disease 2-like 1	−3.47	0.0191	2.34	0.336
MT1L	Metallothionein 1L (gene/pseudogene)	−3.37	0.0006	2.07	0.666
OXTR	Oxytocin receptor	−3.30	0.0464	2.04	0.906
SIGLEC5	Sialic acid-binding Ig-like lectin 5	−3.29	0.0350	2.03	0.912
NCF1	Neutrophil cytosolic factor 1	−3.25	0.0308	2.00	0.987
LRRC39	Leucin rich repeat containing 39	−3.20	0.0082	2.14	0.549

Up- and down-regulated genes by pCRP ($n = 3$) compared to PBS-treated control EPCs were selected based on a Bayesian "volcano plot" of expression with a fold change in expression level greater than twofold, and a p value <0.05 as determined by student's t test

The fold change effect of mCRP treatment, as compared to PBS-treated control EPCs, for the differentially expressed genes was also determined

mCRP, whereas the ability of these cells to support tube formation was significantly reduced after treatment with pCRP, respectively ($p < 0.001$, Fig. 2c).

Differential effect of mCRP and pCRP on the gene expression profile of EPCs

RNA for whole-genome gene expression analysis was extracted after a 72-h culture period of in vitro expanded cord blood-derived $CD34^+$ cells on fibronectin-coated dishes. Cells were treated with mCRP (1 μg/ml), pCRP (5 μg/ml) or PBS in EGM-2. In addition, RNA was extracted before the 72-h culture period to determine the background of differentially expressed genes induced by the EPC differentiation process during the 72-h culture period on fibronectin-coated dishes. The microarray analysis was undertaken in three biological repeats (three different cord blood donors) on beadchips containing >48,000 different probes. Box and whisker plots confirmed that the normalisation of the arrays achieved comparable dynamic range of the different samples (supplementary Fig. 1). In contrast, principal component analysis (PCA) demonstrated that the gene expression, induced by either mCRP or pCRP, was systematically distinct across the three donors (Fig. 3a). Hierarchical clustering of 320 differentially expressed genes further demonstrated that mCRP and pCRP treatment differentially induced coordinate programmatic gene expression and differentiation (Fig. 3b).

The gene expression analysis comparing EPCs treated with mCRP to EPCs treated with PBS detected 42 differentially expressed genes, of which 28 were significantly up-regulated and 14 were down-regulated (at least twofold change, $p < 0.05$) (Table 1). Comparing expression patterns of EPCs treated with pCRP to PBS-treated EPCs detected 86 differentially expressed genes, of which 42 were up-regulated and 44 were down-regulated (at least twofold change, $p < 0.05$) (Table 2). As demonstrated in Table 1, analysis of the differentially expressed genes revealed that mCRP and pCRP showed opposing effects, meaning that the genes up-regulated by mCRP were down-regulated by pCRP, and vice versa.

mCRP, but not pCRP, stimulates the expression of interferon-α responsive genes

To benchmark differential gene expression in EPCs in response to either mCRP or pCRP treatment to existing microarray literature and to gain more biological insight from the gene expression pattern specific for mCRP and pCRP treatment, we have employed Ingenuity Pathway Analysis® (IPA) and Gene Set Enrichment Analysis [41]. Those genes that were up-regulated in response to mCRP exhibited extensive cross interactions, centred around interferon-α (Table 1; Fig. 4). Treatment with pCRP led to a highly different response in the gene expression profile centred around the MAPK pathway, DDIT3/GADD153 and consequent cell growth (ribosomal subunits), and cell cycle regulators such as p21/CDKN1A (Table 2, Fig. 5). Genes with significant down-regulation in response to mCRP and pCRP treatments are described in Tables 1 and 2. An IPA network analysis of selected down-regulated genes in response to mCRP and pCRP, respectively, is depicted in Supplementary Figures 2 and 3.

The gene expression was verified by quantitative real-time PCR with RNA isolated from mCRP (1 μg/ml),

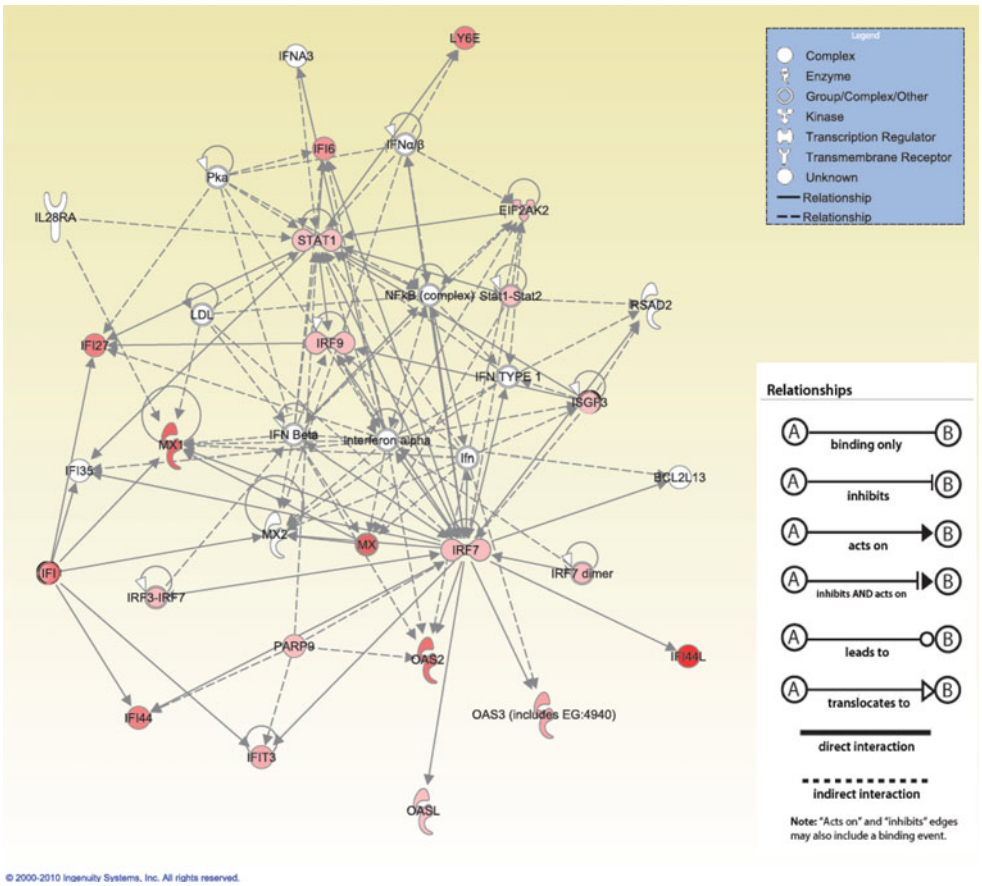

Fig. 4 Ingenuity pathways analysis. Network of up-regulated genes in response to 1 μg/ml mCRP. Networks of gene/gene product interaction were generated using IPA (Ingenuity® Systems, http://www.ingenuity.com). Genes or gene products are represented as nodes, and the biological relationship between two nodes is represented as an *edge* (*line*). All edges are supported by at least one published reference. *Solid edges* represent a direct relationship and *dashed edges* represent an indirect relationship. The *red* node colour represents up-regulation in response to mCRP and the *colour intensity* indicates the degree of up-regulation. The *shape* of each node represents the functional class of the gene product, as shown in the legend

pCRP (5 μg/ml) or PBS-treated EPCs and expressed as fold change in gene expression compared to the PBS-treated control (Fig. 6). Confirming the results of the gene array, IFI44L was the most up-regulated gene in response to mCRP treatment (29.3-fold ± 17) followed by MX1 (8.3-fold ± 2.2) and OAS2 (8.6 ± 2.4) (Fig. 6). Treatment with pCRP but not mCRP led to increased expression of DDIT3 (4.4 ± 0.97) and PROK2 (2.2 ± 0.86) (Fig. 6).

The effects of IFNα2A on phenotypic and functional characteristics of EPCs

The percentage of EPCs double positive for the uptake of AcLDL and binding of ulex lectin was significantly higher ($p < 0.001$) in the presence of IFNα2A or mCRP compared to pCRP (Fig. 7a). Also, compared to pCRP-treated EPCs, IFNα2A or mCRP-treated EPCs gave rise to significantly fewer colonies ($p < 0.01$) (Fig. 7b). Compared to PBS, mCRP or IFNα2A-treated EPCs, pCRP-treated EPCs showed a reduced ability to stimulate endothelial tube formation assessed by the length of endothelial tubes in a Matrigel™ assay with HUVECs (Fig. 7c).

Discussion

This study aimed to assess the effects of pentameric (p)CRP and monomeric (m)CRP on function and differentiation of EPCs. The generation of mCRP by dissociation of pCRP on the cell membrane of activated platelets has been recently described as a pathophysiological mechanism to localise inflammatory reactions, e.g. at developing atherosclerotic plaques [15]. The regenerative capability and the numbers of circulating EPCs have been associated with atherosclerotic plaque development and thus we hypothesised that CRP, particularly mCRP, is a potential regulator of EPC function.

The two major findings of this study are: (1) mCRP and pCRP at concentrations similar to the reported serum levels of CRP in patients with atherosclerotic disease [2] induce an opposing gene expression profile in cord blood-derived EPCs as well as differential effects on the functional capacity of EPCs. (2) The highly up-regulated genes in response to mCRP but not to pCRP treatment are centred around the pro-inflammatory actions of interferon-α and are highly related to up-regulated genes in patients with systemic lupus erythematodes (SLE). Interferon-α2A treatment induced a functional response in EPCs similar to mCRP treatment.

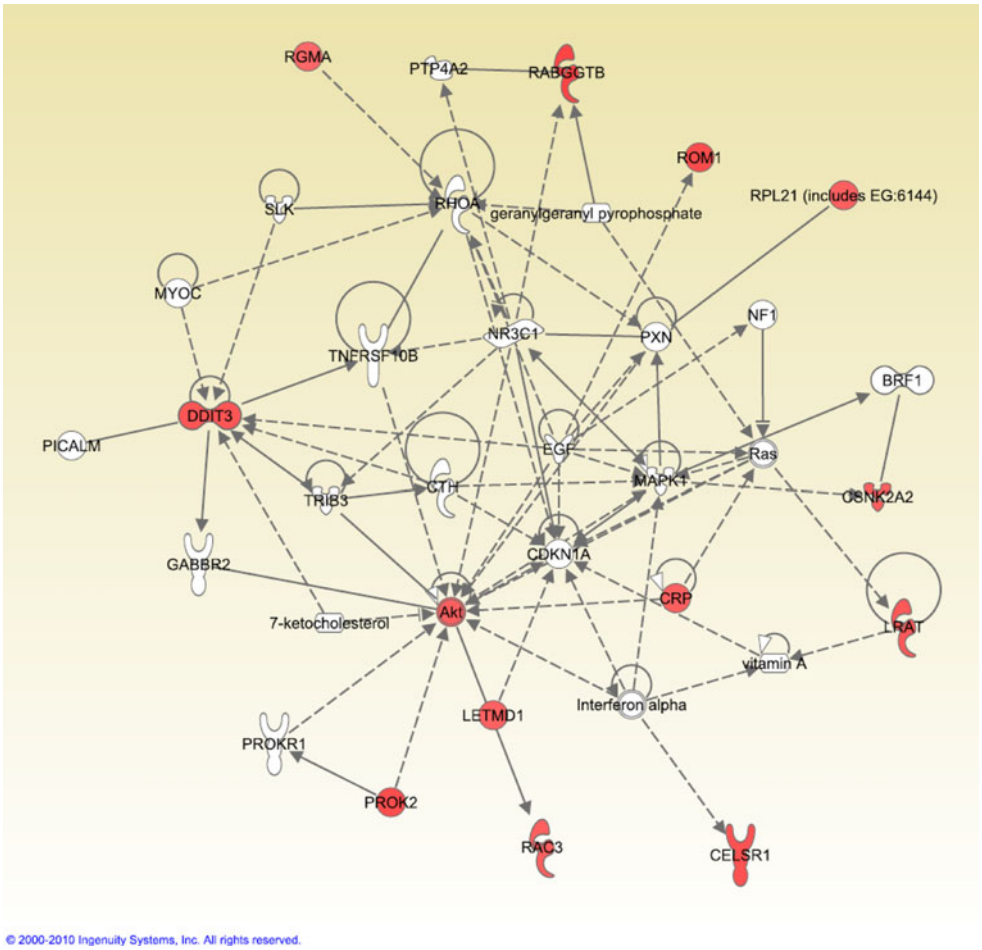

Fig. 5 Ingenuity pathways analysis. Network of up-regulated genes in response to 5 μg/ml pCR*P*. Networks of gene/gene product interaction were generated using IPA (Ingenuity® Systems, http://www.ingenuity.com). Genes or gene products are represented as *nodes*, and the biological relationship between two nodes is represented as an *edge* (*line*). All edges are supported by at least one published reference. *Solid edges* represent a direct relationship and *dashed edges* represent an indirect relationship. The *red* node colour represents up-regulation in response to pCRP. The *shape* of each node represents the functional class of the gene product, as shown in the legend of Fig. 4

Differential effects of mCRP and pCRP on monocyte and platelet function have been observed in previous studies of our group and others [15, 16, 40]. EPC function following pCRP treatment has been extensively examined in previous studies [7, 19, 38, 64], but the differential effects of CRP isoforms on EPCs have not been investigated yet. EPCs are thought to play a key role in the regeneration of injured/inflamed endothelium, and reduced functional capacity of EPCs has been correlated to serum levels of CRP [9]. Therefore, CRP (either monomeric or pentameric) may directly account for the impaired EPC function in patients with chronically elevated serum CRP levels in atherosclerotic disease. Our in vitro study confirms the results of previous studies showing decreased viability and induction of apoptosis with pCRP concentrations >10 μg/ml [5, 19, 52, 64]. Furthermore, we are able to confirm that pCRP, but not mCRP, decreases the number of cells double positive for the uptake of AcLDL and the binding of ulex lectin, which has been described as a common EPC phenotype [24, 29, 48, 69]. The ability of EPCs to stimulate endothelial tube formation in co-cultures with HUVECs has been used to describe the pro-angiogenic functions of EPCs [8, 24, 64]. In line with other reports [64], our results indicate that pCRP directly impairs endothelial tube formation and this occurred at the concentration of 5 μg/ml, which was not cytotoxic to the EPCs, thereby indicating that EPC differentiation rather than viability in response to pCRP treatment impaired the ability of EPCs to support endothelial tube formation. This interpretation is supported by the decreased number of AcLDL and ulex lectin double-positive cells after pCRP treatment and the significant increase in the number of CFU in response to pCRP treatment.

The increase in CFUs may be explained by the up-regulation of two genes (DDIT3 and PROK2) in response to pCRP treatment. PROK2 has been shown to increase the number of CFUs and to enhance progenitor cell mobilisation [36] and DDIT3 (also known as GADD153 or CHOP), although also associated with the response to oxidative stress [12, 42], increased the number of CFUs in erythroid cells [10]. Interestingly, pCRP treatment of human coronary vascular smooth muscle cells with 5 μg/ml of pCRP also led to a >2-fold increase in expression of DDIT3 (GADD153) [5], which has been reproduced by others with higher concentrations of pCRP (25 μg/ml) [52].

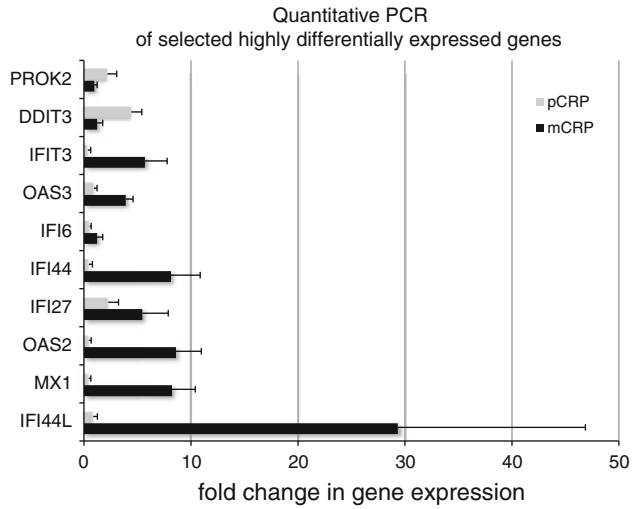

Fig. 6 Validation of the expression of selected highly upregulated genes in mCRP (1 μg/ml) and pCRP (5 μg/ml)-treated EPCs by quantitative real-time PCR. Validation of gene expression by quantitative real-time PCR. The mean in gene expression from EPCs derived from three individual cord blood donors was obtained using differences in cycle threshold between the gene and 18 s (ΔCt). The fold change in difference (ΔΔCt) in gene expression in the treated samples compared to the PBS control samples was determined ($2^{\Delta\Delta Ct}$) and expressed in the diagram as mean and SEM of $n = 3$. *Grey bars* represent pCRP and *black bars* represent mCRP-treated EPCs

In view of our observations showing increased CFUs with low concentrations of pCRP and decreased viability and increased apoptosis with higher concentrations, we hypothesise that moderately elevated levels of pCRP under non-inflammatory conditions may have a different impact on EPC differentiation and function as compared to inflammatory conditions. This is supported by the observation that the endothelial colony forming capacity of EPCs is positively correlated to pCRP levels in healthy volunteers [9]. Whereas under inflammatory conditions, such as those present in atherosclerotic disease, localised dissociation of pCRP to mCRP may occur [15]. This in turn could then have a negative biological effect on EPC numbers and function as observed in patients with atherosclerosis [55, 67, 68].

In our in vitro study, mCRP treatment of EPCs did not decrease the numbers of AcLDL and ulex lectin positive cells and there was also no decrease in their capacity to support endothelial tube formation with mCRP treatment, which furher highlights the differential effects of the two CRP isoforms that has been shown in vitro in various cell types [28, 32–35, 56, 72]. We compared the concentrations of 1 μM mCRP with 5 μM pCRP to account for the differences in molarity between pCRP (115 kDa) and mCRP (23 kDa).

The substantial differences in the effects of mCRP and pCRP were confirmed in whole-genome gene expression analysis. The genes up-regulated by mCRP are known to be responsive to the pro-inflammatory interferon-α. Among the 28 highly up-regulated genes in response to mCRP treatment were nine interferon-inducible genes (IFI44L, MX1, IFI27, OAS3, IFI44, Ly6E, EPISTI1, STAT1). Interestingly, these genes matched highly up-regulated genes described in the microarray analysis of tissue from synovial biopsies of patients with systemic lupus erythematosus [44]. In addition, the three genes that showed the strongest up-regulation in response to mCRP (IFI44L, MX1 and OAS2) were also found to be the most up-regulated genes in peripheral blood mononuclear cells (PBMCs) of paediatric patients with SLE [4]. Importantly, patients with SLE are more prone to the development of atherosclerosis [57] and especially women with SLE and coronary artery disease (CAD) have a poor outcome after percutaneous coronary intervention (PCI) [39]. Interferon-α (measured via expression of the interferon-α responsive genes IFI44 and MX1) has been linked to abnormal vascular repair caused by EPC dysfunction in patients with SLE thereby generating the hypothesis that interferon-α triggered EPC dysfunction is involved in the accelerated atherosclerosis in patients with SLE [11, 30]. This is supported by the observation that increased expression of MX1 in PBMCs of SLE patients and elevated levels of pCRP are independently associated with EPC dysfunction [37]. Furthermore, impaired function of EPCs was accompanied by increased expression of MX1 in an animal model of SLE [60]. Finally, auto-antibodies against mCRP have been described in serum from patients with active SLE [59], which generates the hypothesis that elevated mCRP levels lead to interferon-α-mediated impairment of EPCs in patients with SLE, thereby impairing vascular repair and accelerating the development of atherosclerosis. Of note, our data do not directly demonstrate a pro-atherosclerotic effect of mCRP. However, for interferon-α and β, such a direct pro-atherosclerotic effect has very recently been demonstrated in mouse models of atherosclerosis [21, 43]. Most interestingly, up-regulation of MX1, OAS1, OAS2 and IFIT3 mRNA in ruptured atherosclerotic plaques in human carotid arteries has been found [21].

By confirming the fundamentally different pathological functions of mCRP and pCRP, our findings may help to explain the clinical situation in vivo. The positive impact of pCRP on endothelial colony forming capacity of EPCs observed by us has also been described in healthy volunteers [9]. Under inflammatory conditions, such as atherosclerosis, pCRP is dissociated to mCRP [15] and thus exerts substantially different functions, potentially fuelling the inflammatory response, as suggested by the results of our whole-genome gene expression analysis that suggests pro-inflammatory properties for mCRP. The localised dissociation of pCRP to mCRP in inflammation could

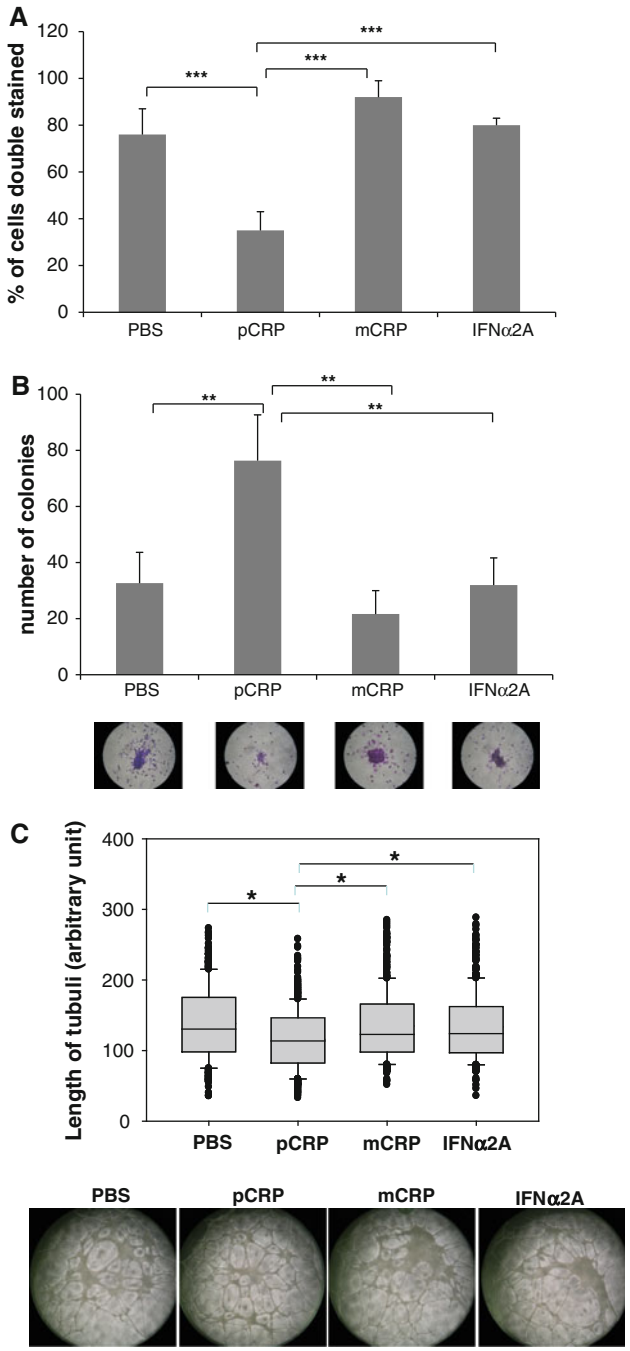

◀ **Fig. 7** The effect of mCRP (1 mg/ml), pCRP (5 mg/ml) or IFNa2A (1 ng/ml) on phenotype and function of EPCs. **a** Binding of ulex lectin and uptake of acetylated LDL after 72 h of culture of EPCs in the presence or absence of pCRP, mCRP and IFNa2A. The *bar graph* shows the percentage of cells double positive for binding of ulex lectin and uptake of acetylated LDL as compared to the total number of cells in three random optical fields (20× magnification). Mean and SD of $n = 3$. The statistical significance was determined by one-way ANOVA with Tukey's post hoc test, ***$p<0.001$. **b** The *bar graph* shows the number of colony forming units (CFU-Hills) visualised by Giemsa staining, formed by EPCs that had been cultured in the presence of pCRP, mCRP or IFNalpha2 for 72 h (mean and SD of three individual donors, $n = 3$). The statistical significance was determined by one-way ANOVA with Tukey's post hoc test, **$p < 0.01$. **c** The *box plot* shows the lengths of the tubuli formed in a co-culture of HUVECs and EPCs ($n = 3$) in an endothelial tube formation assay. The EPCs had been cultured in the presence of pCRP, mCRP or IFNa2A for 72 h prior to the assay. The photomicrographs were taken when a clear tubuli network was observed after 16 h of incubation. The statistical significance was determined by ANOVA on ranks with Dunn's post hoc test, *$p < 0.05$

potentially mediate the negative biological effect on EPC numbers and function observed in patients with atherosclerosis [55, 67, 68].

Our study focussed on the in vitro effects of two isoforms of CRP on cord blood-derived EPCs to explore the functional, phenotypical and gene expression profiles of monomeric and pentameric CRP towards a rare cell population with potent pro-angiogenic capabilities involved in the natural repair of vascular damage. A limitation of our study is that the results obtained in our in vitro system cannot directly be translated into in vivo situation where a more complex system of different vascular cells acts in concert to maintain the vascular integrity, and each cell type may have a different response to the two isoforms of CRP. Furthermore, the use of cord blood-derived cells may bear the risk of a differential response in gene expression in comparison to adult EPCs. However, most of the functional properties of cord blood-derived EPCs resemble those of EPCs derived from adult donors, and EPCs derived from both young and old donors have successfully been used in the past to treat cardiovascular disease in animal models and human subjects [25, 46, 54, 70]. Interestingly, a recent report describes a weaker specific interferon-α-mediated immune response in cord blood-derived mononuclear cells as compared to mononuclear cells from adult donors [65]. Therefore, our gene expression analysis could also underestimate the pro-inflammatory effects of mCRP.

In conclusion, we provide evidence for a differential, highly opposing effect of monomeric and pentameric C-reactive protein on human umbilical cord blood-derived EPCs. Monomeric CRP induced the up-regulation of pro-inflammatory, interferon-responsive genes in EPCs, whereas pentameric CRP exhibited a primarily non-inflammatory gene response. These data support the concept that localised mCRP generation thus provides a means to locally regulate EPC function in vascular homoeostasis.

Acknowledgments This work has been supported by the National Health and Medical Research Council (NHMRC) of Australia (Peter K), the Australian Research Council (future fellowship, Peter K), the German Research Foundation (AH 185/1-1, Ahrens I), the Henning and Johan Throne-Holst's Foundation (Domeij H) and the German Academic Exchange Service DAAD (D/10/47670, Albrecht M). Dr. Martha Lappas is the recipient of an NHMRC RD Wright Fellowship (Grant No. 454777). The authors gratefully acknowledge the

skilful technical assistance of Ruusu-Maria Merivirta, in the stem cell culture; the assistance of the Clinical Research Midwives Gabrielle Fleming, Astrid Tiefholz and Anne Beeston; and the Obstetrics and Midwifery staff of the Mercy Hospital for Women for their co-operation.

References

1. Ahrens I, Domeij H, Topcic D, Mirivirta R, Bode C, Lappas M, Peter K (2010) Successful in vitro expansion and differentiation of cord blood derived CD34+ cells into functionally active endothelial progenitor cells. Eur Heart J 31:279–587 (P2341). doi:10.1093/eurheartj/ehq288
2. Albert MA, Glynn RJ, Ridker PM (2003) Plasma concentration of C-reactive protein and the calculated Framingham Coronary Heart Disease Risk Score. Circulation 108:161–165. doi:10.1161/01.CIR.0000080289.72166.CF
3. Asahara T, Murohara T, Sullivan A, Silver M, van der Zee R, Li T, Witzenbichler B, Schatteman G, Isner JM (1997) Isolation of putative progenitor endothelial cells for angiogenesis. Science 275:964–967. doi:10.1126/science.275.5302.964
4. Bennett L, Palucka AK, Arce E, Cantrell V, Borvak J, Banchereau J, Pascual V (2003) Interferon and granulopoiesis signatures in systemic lupus erythematosus blood. J Exp Med 197:711–723. doi:10.1084/jem.20021553
5. Blaschke F, Bruemmer D, Yin F, Takata Y, Wang W, Fishbein MC, Okura T, Higaki J, Graf K, Fleck E, Hsueh WA, Law RE (2004) C-reactive protein induces apoptosis in human coronary vascular smooth muscle cells. Circulation 110:579–587. doi:10.1161/01.CIR.0000136999.77584.A2
6. Bowman TV, Merchant AA, Goodell MA (2007) Molecular profiling of hematopoietic stem cells. Methods Mol Med 134:1–16. doi:10.1007/978-1-59745-223-6_1
7. Chen J, Huang L, Song M, Yu S, Gao P, Jing J (2009) C-reactive protein upregulates receptor for advanced glycation end products expression and alters antioxidant defenses in rat endothelial progenitor cells. J Cardiovasc Pharmacol 53:359–367. doi:10.1097/FJC.0b013e31819b5438
8. Choi JH, Kim KL, Huh W, Kim B, Byun J, Suh W, Sung J, Jeon ES, Oh HY, Kim DK (2004) Decreased number and impaired angiogenic function of endothelial progenitor cells in patients with chronic renal failure. Arterioscler Thromb Vasc Biol 24:1246–1252. doi:10.1161/01.ATV.0000133488.56221.4a
9. Ciulla MM, Giorgetti A, Silvestris I, Cortiana M, Montelatici E, Paliotti R, Annoni GA, Fiore AV, Giordano R, De Marco F, Magrini F, Rebulla P, Cortelezzi A, Lazzari L (2006) Endothelial colony forming capacity is related to C-reactive protein levels in healthy subjects. Curr Neurovasc Res 3:99–106. doi:10.2174/156720206776875876
10. Coutts M, Cui K, Davis KL, Keutzer JC, Sytkowski AJ (1999) Regulated expression and functional role of the transcription factor CHOP (GADD153) in erythroid growth and differentiation. Blood 93:3369–3378
11. Denny MF, Thacker S, Mehta H, Somers EC, Dodick T, Barrat FJ, McCune WJ, Kaplan MJ (2007) Interferon-alpha promotes abnormal vasculogenesis in lupus: a potential pathway for premature atherosclerosis. Blood 110:2907–2915. doi:10.1182/blood-2007-05-089086
12. Di Nardo A, Kramvis I, Cho N, Sadowski A, Meikle L, Kwiatkowski DJ, Sahin M (2009) Tuberous sclerosis complex activity is required to control neuronal stress responses in an mTOR-dependent manner. J Neurosci 29(18):5926–5937. doi:10.1523/JNEUROSCI.0778-09.2009
13. Dimmeler S (2010) Regulation of bone marrow-derived vascular progenitor cell mobilization and maintenance. Arterioscler Thromb Vasc Biol 30:1088–1093. doi:10.1161/ATVBAHA.109.191668
14. Eisen MB, Spellman PT, Brown PO, Botstein D (1998) Cluster analysis and display of genome-wide expression patterns. Proc Natl Acad Sci USA 95:14863–14868. doi:10.1073/pnas.96.19.10943-c
15. Eisenhardt SU, Habersberger J, Murphy A, Chen YC, Woollard KJ, Bassler N, Qian H, von Zur Muhlen C, Hagemeyer CE, Ahrens I, Chin-Dusting J, Bobik A, Peter K (2009) Dissociation of pentameric to monomeric C-reactive protein on activated platelets localizes inflammation to atherosclerotic plaques. Circ Res 105:128–137. doi:10.1161/CIRCRESAHA.108.190611
16. Eisenhardt SU, Habersberger J, Oliva K, Lancaster GI, Ayhan M, Woollard KJ, Bannasch H, Rice GE, Peter K (2011) A proteomic analysis of C-reactive protein stimulated THP-1 monocytes. Proteome Sci 9:1. doi:10.1186/1477-5956-9-1
17. Eisenhardt SU, Habersberger J, Peter K (2009) Monomeric C-reactive protein generation on activated platelets: the missing link between inflammation and atherothrombotic risk. Trends Cardiovasc Med 19:232–237. doi:10.1016/j.tcm.2010.02.002
18. Friedrich EB, Werner C, Walenta K, Bohm M, Scheller B (2009) Role of extracellular signal-regulated kinase for endothelial progenitor cell dysfunction in coronary artery disease. Basic Res Cardiol 104:613–620. doi:10.1007/s00395-009-0022-6
19. Fujii H, Li SH, Szmitko PE, Fedak PW, Verma S (2006) C-reactive protein alters antioxidant defenses and promotes apoptosis in endothelial progenitor cells. Arterioscler Thromb Vasc Biol 26:2476–2482. doi:10.1161/01.ATV.0000242794.65541.02
20. George J, Goldstein E, Abashidze S, Deutsch V, Shmilovich H, Finkelstein A, Herz I, Miller H, Keren G (2004) Circulating endothelial progenitor cells in patients with unstable angina: association with systemic inflammation. Eur Heart J 25:1003–1008. doi:10.1016/j.ehj.2004.03.026
21. Goossens P, Gijbels MJ, Zernecke A, Eijgelaar W, Vergouwe MN, van der Made I, Vanderlocht J, Beckers L, Buurman WA, Daemen MJ, Kalinke U, Weber C, Lutgens E, de Winther MP (2010) Myeloid type I interferon signaling promotes atherosclerosis by stimulating macrophage recruitment to lesions. Cell Metab 12:142–153. doi:10.1016/j.cmet.2010.06.008
22. Hahne F, Mehrle A, Arlt D, Poustka A, Wiemann S, Beissbarth T (2008) Extending pathways based on gene lists using InterPro domain signatures. BMC Bioinformatics 9:3. doi:10.1186/1471-2105-9-3
23. He LP, Tang XY, Ling WH, Chen WQ, Chen YM (2010) Early C-reactive protein in the prediction of long-term outcomes after acute coronary syndromes: a meta-analysis of longitudinal studies. Heart 96:339–346. doi:10.1136/hrt.2009.174912
24. Hirschi KK, Ingram DA, Yoder MC (2008) Assessing identity, phenotype, and fate of endothelial progenitor cells. Arterioscler Thromb Vasc Biol 28:1584–1595. doi:10.1161/ATVBAHA.107.155960
25. Hu CH, Li ZM, Du ZM, Zhang AX, Rana JS, Liu DH, Yang DY, Wu GF (2010) Expanded human cord blood-derived endothelial progenitor cells salvage infarcted myocardium in rats with acute myocardial infarction. Clin Exp Pharmacol Physiol 37:551–556. doi:10.1111/j.1440-1681.2010.05347.x
26. Huo Y, Schober A, Forlow SB, Smith DF, Hyman MC, Jung S, Littman DR, Weber C, Ley K (2003) Circulating activated platelets exacerbate atherosclerosis in mice deficient in apolipoprotein E. Nat Med 9:61–67. doi:10.1038/nm810
27. Irizarry RA, Hobbs B, Collin F, Beazer-Barclay YD, Antonellis KJ, Scherf U, Speed TP (2003) Exploration, normalization, and

summaries of high density oligonucleotide array probe level data. Biostatistics 4:249–264. doi:10.1093/biostatistics/4.2.249
28. Ji SR, Wu Y, Zhu L, Potempa LA, Sheng FL, Lu W, Zhao J (2007) Cell membranes and liposomes dissociate C-reactive protein (CRP) to form a new, biologically active structural intermediate: mCRP(m). FASEB J 21:284–294. doi:10.1096/fj.06-6722com
29. Jujo K, Ii M, Losordo DW (2008) Endothelial progenitor cells in neovascularization of infarcted myocardium. J Mol Cell Cardiol 45:530–544. doi:10.1016/j.yjmcc.2008.08.003
30. Kaplan MJ (2009) Premature vascular damage in systemic lupus erythematosus. Autoimmunity 42:580–586. doi:10.1080/08916930903002479
31. Kaur S, Kumar TR, Uruno A, Sugawara A, Jayakumar K, Kartha CC (2009) Genetic engineering with endothelial nitric oxide synthase improves functional properties of endothelial progenitor cells from patients with coronary artery disease: an in vitro study. Basic Res Cardiol 104:739–749. doi:10.1007/s00395-009-0039-x
32. Khreiss T, Jozsef L, Hossain S, Chan JS, Potempa LA, Filep JG (2002) Loss of pentameric symmetry of C-reactive protein is associated with delayed apoptosis of human neutrophils. J Biol Chem 277:40775–40781. doi:10.1074/jbc.M205378200
33. Khreiss T, Jozsef L, Potempa LA, Filep JG (2004) Conformational rearrangement in C-reactive protein is required for proinflammatory actions on human endothelial cells. Circulation 109:2016–2022. doi:10.1161/01.CIR.0000125527.41598.68
34. Khreiss T, Jozsef L, Potempa LA, Filep JG (2004) Opposing effects of C-reactive protein isoforms on shear-induced neutrophil-platelet adhesion and neutrophil aggregation in whole blood. Circulation 110:2713–2720. doi:10.1161/01.CIR.0000146846.00816.DD
35. Khreiss T, Jozsef L, Potempa LA, Filep JG (2005) Loss of pentameric symmetry in C-reactive protein induces interleukin-8 secretion through peroxynitrite signaling in human neutrophils. Circ Res 97:690–697. doi:10.1161/01.RES.0000183881.11739.CB
36. LeCouter J, Zlot C, Tejada M, Peale F, Ferrara N (2004) Bv8 and endocrine gland-derived vascular endothelial growth factor stimulate hematopoiesis and hematopoietic cell mobilization. Proc Natl Acad Sci USA 101:16813–16818. doi:10.1073/pnas.0407697101
37. Lee PY, Li Y, Richards HB, Chan FS, Zhuang H, Narain S, Butfiloski EJ, Sobel ES, Reeves WH, Segal MS (2007) Type I interferon as a novel risk factor for endothelial progenitor cell depletion and endothelial dysfunction in systemic lupus erythematosus. Arthritis Rheum 56:3759–3769. doi:10.1002/art.23035
38. Liu C, Wang S, Deb A, Nath KA, Katusic ZS, McConnell JP, Caplice NM (2005) Proapoptotic, antimigratory, antiproliferative, and antiangiogenic effects of commercial C-reactive protein on various human endothelial cell types in vitro: implications of contaminating presence of sodium azide in commercial preparation. Circ Res 97:135–143. doi:10.1161/01.RES.0000174612.90094.fd
39. Maksimowicz-McKinnon K, Selzer F, Manzi S, Kip KE, Mulukutla SR, Marroquin OC, Smitherman TC, Kuller LH, Williams DO, Wasko MC (2008) Poor 1-year outcomes after percutaneous coronary interventions in systemic lupus erythematosus: report from the National Heart, Lung, and Blood Institute Dynamic Registry. Circ Cardiovasc Interv 1:201–208. doi:10.1161/CIRCINTERVENTIONS.108.788745
40. Molins B, Pena E, Vilahur G, Mendieta C, Slevin M, Badimon L (2008) C-reactive protein isoforms differ in their effects on thrombus growth. Arterioscler Thromb Vasc Biol 28:2239–2246. doi:10.1161/ATVBAHA.108.174359
41. Mootha VK, Lindgren CM, Eriksson KF, Subramanian A, Sihag S, Lehar J, Puigserver P, Carlsson E, Ridderstrale M, Laurila E, Houstis N, Daly MJ, Patterson N, Mesirov JP, Golub TR, Tamayo P, Spiegelman B, Lander ES, Hirschhorn JN, Altshuler D, Groop LC (2003) PGC-1alpha-responsive genes involved in oxidative phosphorylation are coordinately downregulated in human diabetes. Nat Genet 34:267–273. doi:10.1038/ng1180
42. Namba T, Tanaka K, Ito Y, Ishihara T, Hoshino T, Gotoh T, Endo M, Sato K, Mizushima T (2009) Positive role of CCAAT/enhancer-binding protein homologous protein, a transcription factor involved in the endoplasmic reticulum stress response in the development of colitis. Am J Pathol 174:1786–1798. doi:10.2353/ajpath.2009.080864
43. Noels H, Weber C (2011) Catching up with important players in atherosclerosis: type I interferons and neutrophils. Curr Opin Lipidol 22:144–145. doi:10.1097/MOL.0b013e328344780b
44. Nzeusseu Toukap A, Galant C, Theate I, Maudoux AL, Lories RJ, Houssiau FA, Lauwerys BR (2007) Identification of distinct gene expression profiles in the synovium of patients with systemic lupus erythematosus. Arthritis Rheum 56:1579–1588. doi:10.1002/art.22578
45. Orlandi A, Chavakis E, Seeger F, Tjwa M, Zeiher AM, Dimmeler S (2010) Long-term diabetes impairs repopulation of hematopoietic progenitor cells and dysregulates the cytokine expression in the bone marrow microenvironment in mice. Basic Res Cardiol 105:703–712. doi:10.1007/s00395-010-0109-0
46. Ott I, Keller U, Knoedler M, Gotze KS, Doss K, Fischer P, Urlbauer K, Debus G, von Bubnoff N, Rudelius M, Schomig A, Peschel C, Oostendorp RA (2005) Endothelial-like cells expanded from CD34+ blood cells improve left ventricular function after experimental myocardial infarction. FASEB J 19:992–994. doi:10.1096/fj.04-3219fje
47. Padfield GJ, Tura O, Haeck ML, Short A, Freyer E, Barclay GR, Newby DE, Mills NL (2010) Circulating endothelial progenitor cells are not affected by acute systemic inflammation. Am J Physiol Heart Circ Physiol 298:H2054–H2061. doi:10.1152/ajpheart.00921.2009
48. Poss J, Werner C, Lorenz D, Gensch C, Bohm M, Laufs U (2010) The renin inhibitor aliskiren upregulates pro-angiogenic cells and reduces atherogenesis in mice. Basic Res Cardiol 105:725–735. doi:10.1007/s00395-010-0120-5
49. Raponi M, Belly RT, Karp JE, Lancet JE, Atkins D, Wang Y (2004) Microarray analysis reveals genetic pathways modulated by tipifarnib in acute myeloid leukemia. BMC Cancer 4:56. doi:10.1186/1471-2407-4-56
50. Richardson MR, Yoder MC (2011) Endothelial progenitor cells: quo vadis? J Mol Cell Cardiol 50:266–272. doi:10.1016/j.yjmcc.2010.07.009
51. Ridker PM, Hennekens CH, Buring JE, Rifai N (2000) C-reactive protein and other markers of inflammation in the prediction of cardiovascular disease in women. N Engl J Med 342:836–843
52. Ryu J, Lee CW, Shin JA, Park CS, Kim JJ, Park SJ, Han KH (2007) FcgammaRIIa mediates C-reactive protein-induced inflammatory responses of human vascular smooth muscle cells by activating NADPH oxidase 4. Cardiovasc Res 75:555–565. doi:10.1016/j.cardiores.2007.04.027
53. Sandstedt J, Jonsson M, Lindahl A, Jeppsson A, Asp J (2010) C-kit+ CD45− cells found in the adult human heart represent a population of endothelial progenitor cells. Basic Res Cardiol 105:545–556. doi:10.1007/s00395-010-0088-1
54. Schachinger V, Erbs S, Elsasser A, Haberbosch W, Hambrecht R, Holschermann H, Yu J, Corti R, Mathey DG, Hamm CW, Suselbeck T, Assmus B, Tonn T, Dimmeler S, Zeiher AM (2006) Intracoronary bone marrow-derived progenitor cells in acute myocardial infarction. N Engl J Med 355:1210–1221. doi:10.1056/NEJMoa060186
55. Schmidt-Lucke C, Rossig L, Fichtlscherer S, Vasa M, Britten M, Kamper U, Dimmeler S, Zeiher AM (2005) Reduced number of

circulating endothelial progenitor cells predicts future cardiovascular events: proof of concept for the clinical importance of endogenous vascular repair. Circulation 111:2981–2987. doi:10.1161/CIRCULATIONAHA.104.504340

56. Schwedler SB, Filep JG, Galle J, Wanner C, Potempa LA (2006) C-reactive protein: a family of proteins to regulate cardiovascular function. Am J Kidney Dis 47:212–222. doi:10.1053/j.ajkd.2005.10.028
57. Sherer Y, Zinger H, Shoenfeld Y (2010) Atherosclerosis in systemic lupus erythematosus. Autoimmunity 43:98–102. doi:10.3109/08916930903374527
58. Steinmetz M, Nickenig G, Werner N (2011) Endothelial-regenerating cells: an expanding universe. Hypertension 55:593–599. doi:10.1161/HYPERTENSIONAHA.109.134213
59. Tan Y, Yu F, Yang H, Chen M, Fang Q, Zhao MH (2008) Autoantibodies against monomeric C-reactive protein in sera from patients with lupus nephritis are associated with disease activity and renal tubulointerstitial lesions. Hum Immunol 69:840–844. doi:10.1016/j.humimm.2008.09.006
60. Thacker SG, Duquaine D, Park J, Kaplan MJ (2010) Lupus-prone New Zealand black/New Zealand white F1 mice display endothelial dysfunction and abnormal phenotype and function of endothelial progenitor cells. Lupus 19:288–299. doi:10.1177/0961203309353773
61. Timmermans F, Plum J, Yoder MC, Ingram DA, Vandekerckhove B, Case J (2009) Endothelial progenitor cells: identity defined? J Cell Mol Med 13:87–102. doi:10.1111/j.1582-4934.2008.00598.x
62. Tsuzuki M (2009) Bone marrow-derived cells are not involved in reendothelialized endothelium as endothelial cells after simple endothelial denudation in mice. Basic Res Cardiol 104:601–611. doi:10.1007/s00395-009-0021-7
63. Van Craenenbroeck EM, Hoymans VY, Beckers PJ, Possemiers NM, Wuyts K, Paelinck BP, Vrints CJ, Conraads VM (2010) Exercise training improves function of circulating angiogenic cells in patients with chronic heart failure. Basic Res Cardiol 105:665–676. doi:10.1007/s00395-010-0105-4
64. Verma S, Kuliszewski MA, Li SH, Szmitko PE, Zucco L, Wang CH, Badiwala MV, Mickle DA, Weisel RD, Fedak PW, Stewart DJ, Kutryk MJ (2004) C-reactive protein attenuates endothelial progenitor cell survival, differentiation, and function: further evidence of a mechanistic link between C-reactive protein and cardiovascular disease. Circulation 109:2058–2067. doi:10.1161/01.CIR.0000127577.63323.24
65. Vosters O, Lombard C, Andre F, Sana G, Sokal EM, Smets F (2010) The interferon-alpha and interleukin-10 responses in neonates differ from adults, and their production remains partial throughout the first 18 months of life. Clin Exp Immunol 162:494–499. doi:10.1111/j.1365-2249.2010.04267.x
66. Walenta KL, Bettink S, Bohm M, Friedrich EB (2010) Differential chemokine receptor expression regulates functional specialization of endothelial progenitor cell subpopulations. Basic Res Cardiol 106:299–305. doi:10.1007/s00395-010-0142-z
67. Werner N, Kosiol S, Schiegl T, Ahlers P, Walenta K, Link A, Bohm M, Nickenig G (2005) Circulating endothelial progenitor cells and cardiovascular outcomes. N Engl J Med 353:999–1007. doi:10.1056/NEJMoa043814
68. Werner N, Nickenig G (2006) Clinical and therapeutical implications of EPC biology in atherosclerosis. J Cell Mol Med 10:318–332. doi:10.1111/j.1582-4934.2006.tb00402.x
69. Yoder MC (2009) Defining human endothelial progenitor cells. J Thromb Haemost 7(Suppl 1):49–52. doi:10.1111/j.1538-7836.2009.03407.x
70. Yu Y, Gao Y, Qin J, Kuang CY, Song MB, Yu SY, Cui B, Chen JF, Huang L (2010) CCN1 promotes the differentiation of endothelial progenitor cells and reendothelialization in the early phase after vascular injury. Basic Res Cardiol 105:713–724. doi:10.1007/s00395-010-0117-0
71. Zimmermann O, Bienek-Ziolkowski M, Wolf B, Vetter M, Baur R, Mailander V, Hombach V, Torzewski J (2009) Myocardial inflammation and non-ischaemic heart failure: is there a role for C-reactive protein? Basic Res Cardiol 104:591–599. doi:10.1007/s00395-009-0026-2
72. Zouki C, Haas B, Chan JS, Potempa LA, Filep JG (2001) Loss of pentameric symmetry of C-reactive protein is associated with promotion of neutrophil–endothelial cell adhesion. J Immunol 167:5355–5361